Nanoscale optical biosensors based on localized surface plasmon resonance spectroscopy

Amanda J. Haes and Richard P. Van Duyne
*Department of Chemistry, Northwestern University, 2145 Sheridan Road, Evanston, IL USA 60208-3113

ABSTRACT

The Ag nanoparticle based localized surface plasmon resonance (LSPR) nanosensor yields ultrasensitive biodetection with extremely simple, small, light, robust, and low-cost instrumentation. Using LSPR spectroscopy, the model system, biotinylated surface-confined Ag nanotriangles, was used to detect less than one picomolar up to micromolar concentrations of streptavidin. Additionally, the monitoring of anti-biotin binding to biotinylated Ag nanotriangles exhibited that the system could be used as a solution immunoassay. The system was rigorously tested for nonspecific binding interactions and was found to display virtually no adverse results. These results represent important new steps in the development of the LSPR nanobiosensor for applications in medical diagnostics, biomedical research, and environmental science.

Keywords: Plasmon resonance, nanosphere lithography, nanoparticles, biosensors, streptavidin, anti-biotin

1. INTRODUCTION

The development of biosensors for the diagnosis and monitoring of diseases, drug discovery, proteomics, and the environmental detection of pollutants and/or biological agents is an extremely significant problem.[1] Fundamentally, a biosensor is derived from the coupling of a ligand-receptor binding reaction[2] to a signal transducer. Much biosensor research has been devoted to the evaluation of the relative merits of various signal transduction methods including optical,[3, 4] radioactive,[5, 6] electrochemical,[7, 8] piezoelectric,[9, 10] magnetic,[11, 12] micromechanical,[13, 14] and mass spectrometric.[15, 16] The development of large-scale biosensor arrays composed of highly miniaturized signal transducer elements that enable the real-time, parallel monitoring of multiple species is an important driving force in biosensor research.

Recently, several research groups have begun to explore alternative strategies for the development of optical biosensors[17-35] and chemosensors[17, 36-41] based on the extraordinary optical properties of noble metal nanoparticles. Recently, we demonstrated that nanoscale chemosensors and biosensors could be realized through shifts in the localized surface plasmon resonance (LSPR) extinction maximum (λ_{max}) of triangular silver nanoparticles.[17, 42-44] These wavelength shifts are caused by adsorbate-induced local refractive index changes in competition with charge-transfer interactions at the surfaces of nanoparticles.

The nanoscale biosensor based on LSPR spectroscopy operates in a manner totally analogous to propagating surface plasmon resonance (SPR) sensors by transducing small changes in refractive index near the noble metal surface into a measurable wavelength shift response.[17, 42-44] The response of the LSPR and SPR sensors, ΔR_{max}, can be described by the following equation:[42, 45]

$$\Delta R_{max} = m(n_{adsorbate} - n_{blank})\left[\exp\left(-\frac{2d_{adsorbate}}{l_d}\right)\right]\left[1-\exp\left(-\frac{2d_{adsorbate}}{l_d}\right)\right] \quad (1)$$

* vanduyne@chem.northwestern.edu; phone 1 847 491-3516; fax 1 847 491-4530; www.chem.northwestern.edu/~vanduyne

where m is the refractive index sensitivity of the sensor, $n_{adsorbate}$ and n_{blank} are the refractive indexes of the desired adsorbate and bulk environment prior to the sensing event, respectively, $d_{adsorbate}$ is the effective thickness of the adsorbate layer, and l_d is the characteristic electromagnetic field decay length associated with the sensor. While the response of the LSPR and SPR sensors can be derived via the same equation, the sensitivities of the two techniques arise from different experimental parameters. Flat surface SPR sensors have a large refractive index sensitivity, ~$2x10^6$ nm/RIU, and their sensitivity arises primarily from this large value.[45-48] LSPR nanosensors have a modest refractive index sensitivity, ~$2x10^2$ nm/RIU.[17] Despite the smaller refractive index sensitivity of the LSPR nanosensor in comparison to the SPR sensor, both have approximately equivalent behaviors for a given adsorbate. For an identical sensing system, the only other variable (the first being refractive index sensitivity) that varies between the two systems is the electromagnetic field decay length, l_d. SPR sensors have a decay length on the order of ~200 nm.[45] For the nanoparticles described here and the corresponding LSPR nanosensor, a much shorter electromagnetic field decay length (~6 nm) has been measured.[49] This short decay length gives rise to the large sensitivity of the LSPR nanosensor.[42]

The platform employed for synthesis of these nanoparticle-based sensors is known as nanosphere lithography (NSL). NSL is a powerful fabrication technique to inexpensively produce nanoparticle arrays with controlled shape, size, and interparticle spacing.[50] The need for monodisperse, reproducible, and materials general nanoparticles has driven the development and refinement of the most basic NSL architecture as well as many new nanostructure derivatives. Every NSL structure begins with the self-assembly of size-monodisperse nanospheres of diameter D to form a two-dimensional colloidal crystal deposition mask. Methods for deposition of a nanosphere solution onto the desired substrate include spin coating,[50] drop coating,[51] and thermoelectrically-cooled angle coating.[52] All of these deposition methods require that the nanospheres be able to freely diffuse across the substrate seeking their lowest energy configuration. This is often achieved by chemically modifying the nanosphere surface with a negatively charged functional group such as carboxylate or sulfate that is electrostatically repelled by the negatively charged surface of a substrate such as mica or glass. As the solvent (water) evaporates, capillary forces draw the nanospheres together, and the nanospheres crystallize in a hexagonally close-packed pattern on the substrate. As in all naturally occurring crystals, nanosphere masks include a variety of defects that arise as a result of nanosphere polydispersity, site randomness, point defects (vacancies), line defects (slip dislocations), and polycrystalline domains. Typical defect-free domain sizes are in the 10 - 100 μm range. Following self-assembly of the nanosphere mask, a metal or other material is then deposited by thermal evaporation, electron beam deposition, or pulsed laser deposition from a collimated source normal to the substrate through the nanosphere mask to a controlled mass thickness, d_m. After metal deposition, the nanosphere mask is removed, typically by sonicating the entire sample in a solvent, leaving behind the material deposited through the nanosphere mask and onto the substrate.

Previously, we have considerably optimized the LSPR biosensor design by increasing nanoparticle adhesion.[44] First, the NSL sphere packing technique was modified by changing the sample substrate from glass to mica and by adding a surfactant, Triton X-100 and methanol (1:400 by volume) in a 1:1 ratio to the sphere solution before drop coating. The resulting surface area of a perfect single layer sphere monolayer is increased, and as a result, the number of monodisperse Ag nanoparticles in that area is increased. The change in substrate and the use of a surfactant have also dramatically improved the adhesion of the Ag nanoparticles to the sensor substrate. It was shown that a normal force of 10 nN, as determined by atomic force microscopy (AFM), was sufficient to remove all Ag nanoparticles from a glass surface. By performing the force measurements on mica substrates where no surfactant was used, it was revealed that the normal force required to remove the nanoparticles increased to 50 nN. The mechanical stability, or adhesion of the nanoparticles onto mica, increased even further to 90 nN of normal force when Triton X-100 was used during sphere packing. The LSPR biosensor now fulfills two major prerequisites for biological studies; that is, it is robust and durable. Two additional factors that are indispensable for *in vivo* use of a nanobiosensor are effectiveness under physiological conditions and reusability. We demonstrate that for the anti-biotin/biotin model, the LSPR biosensor works in 10 mM phosphate buffered saline (PBS), a close emulate of physiological fluids,[53] with a loss of sensitivity less than that expected from theoretical studies.[42]

In this paper, the extreme sensitivity of Ag nanoparticles to their dielectric environment will be exhibited through the quantitative detection of the tetrameric protein, streptavidin and of the immunoglobulin, anti-biotin. Detection comparisons will be made for a full monolayer coverage of the given molecules. Additionally, detection limits of

the two systems will be compared and a mathematical interpretation of the results will be summarized. Finally, exciting advances in nanoparticle adhesion will be displayed and proven via a reversible, in solution immunoassay.

2. METHODOLOGY AND MATERIALS

2.1 Materials

11-Mercaptoundecanoic acid (11-MUA), 1-octanethiol (1-OT), hexanes, and methanol were purchased from Aldrich (Milwaukee, WI). Anti-biotin, 1-ethyl-3-[3-dimethylaminopropyl]carbodiimide hydrochloride (EDC), streptavidin, 10 mM and 20 mM phosphate buffered saline (PBS) pH=7.4 was obtained from Sigma (St. Louis, MO). (+)-Biotinyl-3,6-dioxaoctanediamine (biotin) was purchased from Pierce (Rockford, IL). Absolute ethanol was purchased from Pharmco (Brookfield CT). Ag wire (99.95%, 0.5 mm) was purchased from D. F. Goldsmith (Evanston, IL). Borosilicate glass substrates were purchased from Fisher Scientific (Pittsburgh, PA). Ruby red muscovite mica substrates were purchased from Asheville-Schoonmaker Mica Co. (Newport News, VA). Polystyrene nanospheres with diameters of 400±7 nm and 390±19.5 nm (Interfacial Dynamics, Portland, OR; Duke Scientific, Long Beach, CA, respectively) were received as a suspension in water. All materials were used without further purification.

2.2 Substrate Preparation

Glass substrates were cleaned in a piranha solution (1:3 30%H_2O_2:H_2SO_4) at 80°C for 30 minutes. Once cooled, the glass substrates were rinsed with copious amounts of water and then sonicated for 60 minutes in 5:1:1 H_2O:NH_4OH:30%H_2O_2. Next the glass was rinsed repeatedly with water and was stored in water until used.

Mica substrates with a 0.003" thickness were cut into 18 mm diameter circles. The samples were freshly cleaved immediately before use.

2.3 Nanoparticle Preparation

NSL was used to fabricate monodisperse, surface-confined triangular Ag nanoparticles. A solution of nanospheres was drop coated onto a clean substrate and allowed to self-assemble into a 2D hexagonally close packed array that served as a deposition mask. On mica, the original nanosphere solution was diluted as a 1:1 solution with Triton X-100 and methanol (1:400 by volume). Approximately 4 μL of this solution produced large areas of single layer colloidal crystal nanosphere masks. The surfactant allowed for better packing of the nanospheres on the mica surface. On glass, single layer colloidal crystal nanosphere masks were prepared by drop coating ~2 μL of undiluted nanosphere solution on glass and mica substrates. The samples were then mounted into a Consolidated Vacuum Corporation vapor deposition chamber system. A Leybold Inficon XTM/2 quartz crystal microbalance (East Syracuse, NY) was used to monitor the thickness of the Ag film deposited on the nanosphere mask. All samples in this study were covered with 50.0 nm thickness Ag films. Following Ag vapor deposition, the nanosphere mask was removed by sonicating the samples in ethanol for 3 minutes.

2.4 Ultraviolet-visible Extinction Spectroscopy

Macroscale UV-visible extinction measurements were collected using an Ocean Optics spectrometer. All spectra collected are macroscopic measurements performed in standard transmission geometry with unpolarized light. The probe beam diameter was approximately 4 mm.

2.5 Experimental Setup and Nanoparticle Functionalization

A home built flow cell was used to control the external environment of the Ag nanoparticle substrates (Figure 1). Prior to modification, the Ag nanoparticles were solvent annealed with hexanes and methanol. Dry N_2 gas and solvent were cycled through the flow cell until the λ_{max} of the sample stabilized. Self-assembled monolayers

(SAMs) composed of a 3:1 ratio of 1-OT:11-MUA in ethanol formed on the samples over 18-36 hours. Next, biotin was linked to the surface over a three hour time period via incubation in a 1:1 ratio of EDC:biotin in 10 mM PBS.

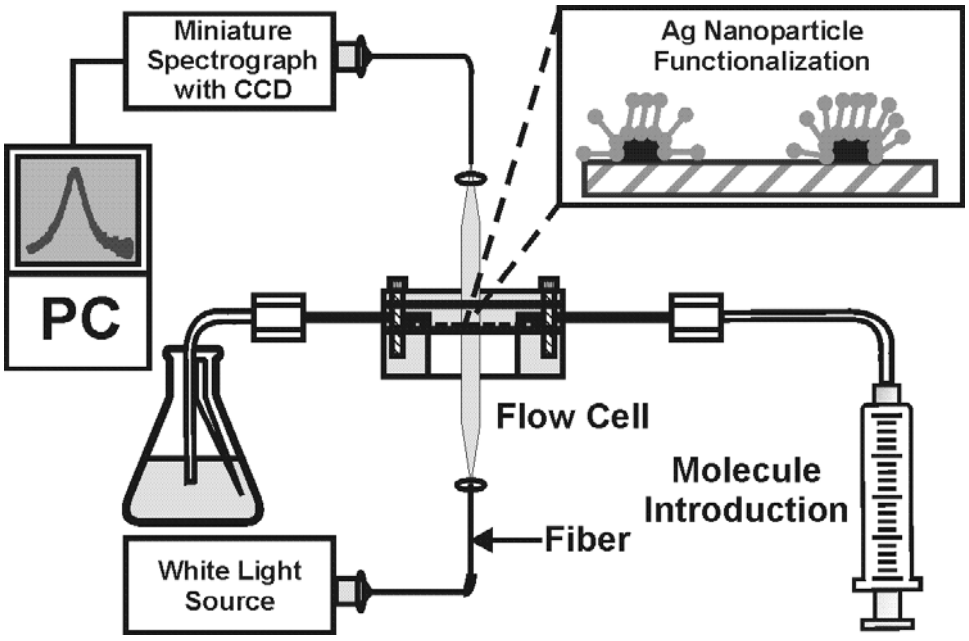

Figure 1. Instrumental diagram for the LSPR nanosensor experiment. The flow cell is fiber optically coupled to a white light source and miniature spectrometer. The cell is directly linked to either a solvent reservoir or to a syringe containing the desired analyte.

Samples were then incubated in a given concentration of streptavidin or anti-biotin in PBS for three hours. Samples were rinsed thoroughly with 10 mM and 20 mM PBS after biotinylation and after detection of streptavidin or anti-biotin to ensure removal of non-specifically bound materials.

2.6 Atomic Force Microscopy (AFM)

A Digital Instruments Nanoscope IV microscope with a Nanoscope IIIa controller operating in either contact or tapping mode was used to collect AFM images in ambient conditions. In tapping mode, etched Si nanoprobe tips (TESP, Digital Instruments, Santa Barbara, CA) were used. These tips had resonance frequencies between 280 and 320 kHz and are conical in shape, with a cone angle of 20° and an effective radius of curvature at the tip of 10 nm. All images shown are unfiltered data that were collected in ambient conditions.

3. RESULTS AND DISCUSSION

3.1 Streptavidin Sensing using LSPR Spectroscopy

The well-studied biotin-streptavidin system with its extremely high binding affinity (K_a~10^{13} M^{-1})[54] is chosen to illustrate the attributes of these LSPR based nanoscale affinity biosensors. The biotin-streptavidin system has been studied in great detail by SPR spectroscopy[48, 55] and serves as an excellent model system for the LSPR nanosensor.[42, 56] Streptavidin, a tetrameric protein, can bind up to four biotinylated molecules (i.e. antibodies, inhibitors, nucleic acids, etc.) with minimal impact on its biological activity[56] and, therefore, will provide a ready pathway for extending the analyte accessibility of the LSPR nanobiosensor.

NSL was used to create surface-confined triangular Ag nanoparticles supported on a glass substrate (Figure 2A). The Ag nanotriangles have in-plane widths of ~ 100 nm and out-of-plane heights of ~ 51 nm as determined by

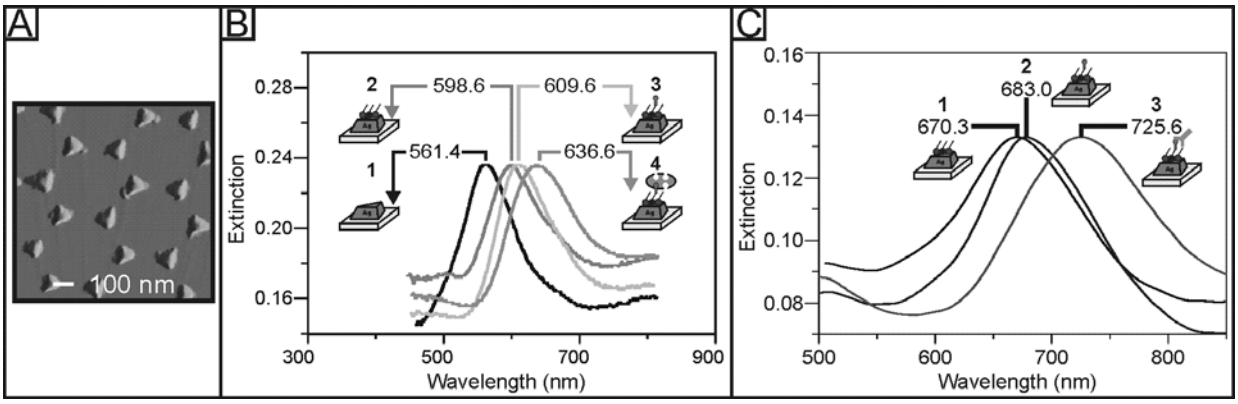

Figure 2. (A) Tapping mode AFM image of Ag nanoparticles (in-plane width~90 nm, out-of-plane widths~50 nm Ag on a mica substrate). Scan area, 1.0 μm^2. (B) LSPR spectra of each step in the surface modification of NSL-derived Ag nanoparticles to form a biotinylated Ag nanobiosensor and the specific binding of streptavidin. (1) Ag nanoparticles before chemical modification, λ_{max} = 561.4 nm. (2) Ag nanoparticles after modification with 1 mM 1:3 11-MUA:1-OT, λ_{max} = 598.6 nm. (3) Ag nanoparticles after modification with 1 mM biotin, λ_{max} = 609.6 nm. (4) Ag nanoparticles after modification with 100 nM streptavidin, λ_{max} = 636.6 nm. All extinction measurements were collected in a N_2 environment. (C) Smoothed LSPR spectra for each step of the preparation of the Ag nanobiosensor, and the specific binding of anti-biotin to biotin. (1) Ag nanoparticles after modification with 1 mM 3:1 1-OT/11-MUA, λ_{max} = 670.3 nm, (2) Ag nanoparticles after modification with 1 mM biotin, λ_{max} = 683.0 nm, and (3) Ag nanoparticles after modification with 700 nM anti-biotin, λ_{max} = 725.6 nm. All spectra were collected in a N_2 environment.

AFM. To prepare the LSPR nanosensor for biosensing events, the Ag nanotriangles are first functionalized with a self-assembled monolayer (SAM) composed of 3:1 1-OT:11-MUA resulting in a surface coverage corresponding to 0.1 monolayer of carboxylate binding sites. Since the maximum number of alkanethiol molecules per nanoparticle is 60,000, this is equivalent to ~ 6000 carboxylate binding sites per nanoparticle. Next, biotin was covalently attached to the carboxylate groups using a zero-length coupling reagent. The number of resulting biotin sites will be determined by the yield of this
coupling reaction. Since this is likely to be ~1-5% efficient one expects there to be only 60-300 biotin sites per nanoparticle at maximum coverages.

Before surface functionalization, the Ag nanoparticles were exposed to solvent and N_2 as described above. In this study, the λ_{max} of the Ag nanoparticles were monitored during each surface functionalization step (Figure 2B). First, the LSPR λ_{max} of the bare Ag nanoparticles was measured to be 561.4 nm (Figure 2B-1). To ensure a well-ordered SAM on the Ag nanoparticles, the sample was incubated in the thiol solution for 24 hours. After careful rinsing and thorough drying with N_2 gas, the LSPR λ_{max} after modification with the mixed SAM (Figure 2B-2) was measured to be 598.6 nm. The LSPR λ_{max} shift corresponding to this surface functionalization step was a 38 nm red-shift, hereafter + will signify a red-shift and - a blue-shift, with respect to bare Ag nanoparticles. Next, biotin was covalently attached via amide bond formation with a two unit polyethylene glycol linker to carboxylated surface sites. The LSPR λ_{max} after biotin attachment (Figure 2B-3) was measured to be 609.6 nm corresponding to an additional + 11 nm shift. The LSPR nanosensor has now been prepared for exposure to the target analyte. Exposure to 100 nM streptavidin, resulted in LSPR λ_{max} = 636.6 nm (Figure 2B-4) corresponding to an additional +27 nm shift. It should be noted that the signal transduction mechanism in this nanosensor is a reliably measured wavelength shift rather than an intensity change as in many previously reported nanoparticle-based sensors.

3.2 Anti-biotin Sensing using LSPR Spectroscopy

A field of particular interest is the study of the interaction between antigens and antibodies.[57] For these reasons we have chosen to focus the present LSPR nanobiosensor study on the prototypical immunoassay involving biotin and anti-biotin, an IgG antibody. In this study, we report the use of Ag nanotriangles synthesized using NSL as a LSPR biosensor that monitors the interaction between a biotinylated surface and free anti-biotin in solution.[44] The importance of this study is that it demonstrates the feasibility of LSPR biosensing with a biological couple whose binding affinity is significantly lower ($1.9x10^6$ - $4.98x10^8$ M^{-1})[58, 59] than in the biotin/streptavidin model.

NSL was used to create massively parallel arrays of Ag nanotriangles on a mica substrate. A SAM of 1:3 1-MUA:1-OT was formed on the surface by incubation for 24 hours. As in the streptavidin experiments, a zero length coupling agent was then used to covalently link biotin to the carboxylate groups.

Each step of the functionalization of the samples was monitored using UV-vis spectroscopy, as shown in Figure 2C. After a 24 hour incubation in SAM, the LSPR extinction wavelength of the Ag nanoparticles was measured to be 670.3 nm (Figure 2C-1). Samples were then incubated for 3 hours in biotin to ensure that the amide bond between the amine and carboxyl groups had been formed. The LSPR wavelength shift due to this binding event was measured to be +12.7 nm, resulting in a LSPR extinction wavelength of 683.0 nm (Figure 2C-2). At this stage, the nanosensor was ready to detect the specific binding of anti-biotin. Incubation in 700 nM anti-biotin for three hours resulted in a LSPR wavelength shift of + 42.6 nm, giving a λ_{max} of 725.6 nm (Figure 2C-3).

3.3 Monitoring the Specific Binding of Streptavidin to Biotin and Anti-Biotin

The well-studied biotin/streptavidin[49] system with its extremely high binding affinity (K_a ~10^{13} M^{-1}) and the antigen-antibody couple, biotin/anti-biotin (K_a ~ 10^6 – 10^8 M^{-1})[44] have been chosen to illustrate the attributes of these LSPR-based nanoscale affinity biosensors. The LSPR λ_{max} shift, ΔR, vs. [analyte] response curve was measured over the concentration range $1x10^{-15}$ M < [streptavidin] < $1x10^{-6}$ M and $7x10^{-10}$ M < [anti-biotin] < $7x10^{-6}$ M (Figure 3).[44, 49] Each data point is an averaged resulted from the analysis of three different samples at identical concentrations. The lines are not a fit to the data. Instead, the line was computed from a response model[44] described by

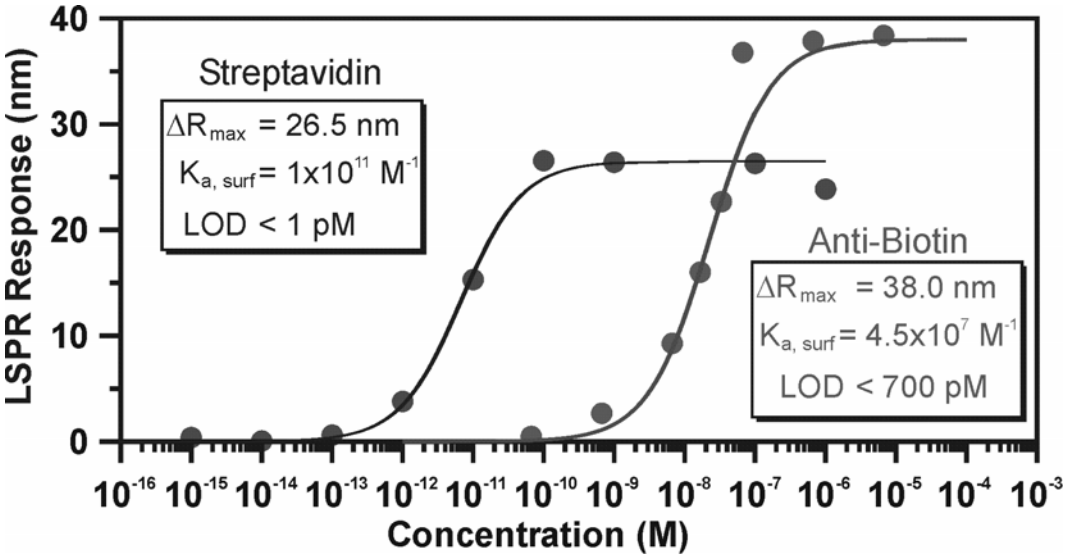

Figure 3. The specific binding of streptavidin (left) and anti-biotin (right) to a biotinylated Ag nanobiosensor is shown in the response curves. All measurements were collected in a N_2 environment. The solid line is the calculated value of the nanosensor's response.

$$\Delta R=\Delta R_{max}\left(\frac{K_{a,surf}[Analyte]}{1+K_{a,surf}[Analyte]}\right) \quad (2)$$

where ΔR is the nanosensor's response for a given analyte concentration, [Analyte], ΔR_{max} is the maximum sensor response for a full monolayer coverage, and $K_{a,surf}$ is the surface confined binding constant. It was found that this response could be interpreted quantitatively in terms of a model involving: (1) 1:1 binding of a ligand to a multivalent receptor with different sites but invariant affinities and (2) the assumption that only adsorbate-induced local refractive index changes were responsible for the operation of the LSPR nanosensor.
The binding curve provides three important characteristics regarding the system being studied. First, the mass and dimensions of the molecules affect the magnitude of the LSPR shift response. Comparison of the data with theoretical expectations yielded a saturation response, ΔR_{max} = 26.5 nm for streptavidin, a 60 kDa molecule, and 38.0 nm for anti-biotin, a 150 kDa molecule. Clearly, a larger mass density at the surface of the nanoparticle results in a larger LSPR response. Next, the surface-confined thermodynamic binding constant $K_{a,surf}$ can be calculated from the binding curve and is estimated to be $1x10^{11}$ M^{-1} for streptavidin and $4.5x10^{7}$ M^{-1} for anti-biotin. These numbers are directly correlated to the third important characteristic of the system, the limit of detection (LOD). The LOD is less than 1 pM for streptavidin and 100 pM for anti-biotin. As predicted, the LOD of the nanobiosensor studied is lower for systems with higher binding affinities such as for the well-studied biotin-streptavidin couple and higher for systems with lower binding affinities as seen in the anti-biotin system.

3.4 Reversibility

In order for LSPR nanobiosensors to fulfill their mandate, they must be biocompatible and work under physiological conditions. Some binding interactions such as poly-L-lysine to a negatively charged surface can interact reversibly, while other couples with higher surface binding affinities interact irreversibly. A commercially viable nanobiosensor should be entirely reusable. In the case of this study, this means that the analyte detection must be entirely removable rendering the sensor reusable. Reusability has a large impact on cost effectiveness and the simplicity of use of biosensors.

The reversibility of the binding between anti-biotin and biotin was tested experimentally by exposing an anti-biotin functionalized sample to an excess of concentrated biotin (1 mM in 10 mM buffer) (Figure 4). The empty binding

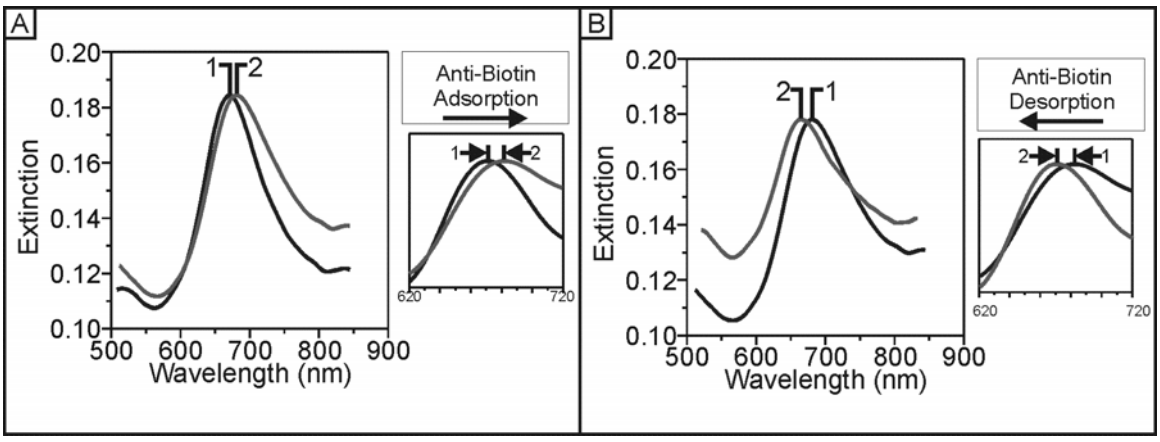

Figure 4. Smoothed LSPR spectra showing the adsorption/desorption of 20 nM anti-biotin to biotinylated Ag nanoparticles. (A) Anti-biotin adsorption: (1) LSPR spectrum of biotinylated Ag nanoparticles in 10 mM PBS, λ_{max} = 671.1 nm, (2) LSPR spectrum of Ag nanoparticles after incubation in 20 nM anti-biotin in 10 mM PBS, λ_{max} = 681.8 nm. (B) Anti-biotin desorption: (2) LSPR spectrum of biotinylated Ag nanoparticles after incubation in 20 nM anti-biotin in 10 mM PBS, λ_{max} = 681.8 nm, (2) LSPR spectrum of Ag nanoparticles after incubation in an excess of biotin (1 mM) in 10 mM PBS for 30 seconds, λ_{max} = 670.2 nm.

sites on the anti-biotin molecules make the molecule susceptible to removal in these conditions. The LSPR spectra[44] of a sample before treatment with anti-biotin revealed a λ_{max} = 671.1 nm (Figure 4A-1). After incubation in 20 nM anti-biotin for three hours, the LSPR extinction wavelength was λ_{max} = 681.8 nm, a shift of +10.7 nm (Figure 4A-2). After 30 seconds of exposure to the 1 mM biotin, the LSPR extinction wavelength λ_{max} blue-shifted to 670.2 nm, a shift of -11.6 nm (Figure 4B). Considering sensor limitations, this value of λ_{max} is essentially identical to its value before treatment with anti-biotin suggesting that the analyte layer had been completely removed. All measurements were made in 10 mM buffer to ensure the applicability of the results to biological sensing. In order to fully understand this phenomenon, real time kinetic studies of the binding and desorption of anti-biotin and the adsorption of biotin to the nanoparticle surface must be performed. The time scale for these events appears to be less than a minute, except for the coupling of EDC, which is significantly slower. Such studies would also reveal useful kinetic data about the interaction of biotin and the analyte,[46, 47, 60, 61] and would provide a supplementary tool to measure the surface binding affinity between the two.

3.5 Selectivity

Although LSPR spectroscopy is a totally nonselective sensor platform, a high degree of analyte selectivity can be conferred using the specificity of surface-attached ligands and passivation of the sensor surface to nonspecfic binding. For this reason, a set of control experiments were performed to show that the streptavidin and anti-biotin binding to the sensor surface containing no capture ligand (biotin), pre-biotinylated streptavidin binding to a sensor surface with biotin, and bovine serum albumin in large excess, simulating a clinical sample, binding to a sensor surface with biotin all produce wavelength shift responses less than that corresponding to the LOD.[44]

4. CONCLUSIONS

Our results suggest that in the near future, Ag nanotriangle biosensors could be used for the detection of a wide variety of biomolecules. Binding of DNA,[20] proteins,[62] and possibly eukaryotic cells (by using protein ligand intermediates) to noble metal nanoparticles opens a window of opportunity in medical diagnostics and could greatly simplify often tedious immunohistochemical detection tasks[63] performed regularly in biomedical research. Future work on miniaturization of the sensor, linkage of the sensor to drug delivery chips, and biocompatibility could make this laboratory based device into a portable diagnostic tool. The simplicity, durability, and reusability of the LSPR nanobiosensor announce its potential use as an affordable and efficient medical device.

In this study, we report the use of Ag nanotriangles synthesized using NSL[64] as a LSPR biosensor that monitors the interaction between a biotinylated surface and free streptavidin or anti-biotin in solution. The importance of this study is that it demonstrates the feasibility of LSPR biosensing for biological couples whose binding affinity ranges from $10^{13} - 10^{15}$ M^{-1} for streptavidin to significantly lower levels ($1.9x10^{6}$ - $4.98x10^{8}$ M^{-1}) for anti-biotin. The biotin-streptavidin model demonstrated that LSPR biosensing was possible in nitrogen conditions. The anti-biotin study expands on the streptavidin work and also demonstrates the use of LSPR nanobiosensing under biologically relevant conditions. While this LSPR biosensor functions analogously to the one used for the streptavidin model, differences were noticed and improvements were made to its setup. Namely, changes were seen in the maximum LSPR response, as expected since this depends on the size and density of the analyte molecule; the surface binding affinity for the anti-biotin/biotin pair; and the limit of detection of the biosensor (directly dependent on the binding affinity constant). The maximum LSPR wavelength shift observed for streptavidin binding to biotinylated nanoparticles was $\Delta\lambda_{max}$ = +26.5 nm and for anti-biotin binding to biotinylated nanoparticles was $\Delta\lambda_{max}$ = +38.0 nm. Fits to the experimental data revealed a surface binding affinity of $4.5x10^{7}$ M^{-1} for the binding of anti-biotin to the biotinylated Ag nanoparticles and $1x10^{11}$ M^{-1} for the binding of streptavidin to the biotinylated Ag nanoparticles. Finally, the limit of detection for the biosensor was determined to be less than 700 pM anti-biotin, which as predicted, is higher than that observed for streptavidin which interacts very strongly with biotin. Finally, it has been shown that by treating samples that have anti-biotin on them with an excess of concentrated biotin, the binding of anti-biotin to the biotinylated Ag nanoparticles can be completely reversed, rendering the sample reusable. These results, in combination with previous studies that indicated that the LSPR nanobiosensor reacts minimally to nonspecific binding,[42] offer an exciting application of nanoscience to medical diagnostics and biomedical research.

The LSPR nanobiosensor developed in this study is expected to demonstrate a wide range of biomedical and environmental applications. Its simplicity and low cost will make it accessible to the public, which could revolutionize medical diagnostics and medical economics. Presently, work is being done to miniaturize the LSPR biosensor to monitor single molecule binding events on single nanoparticles.[65] Increasing the speed of adsorption and desorption of the analyte to the biotinylated surface would offer the possibility of real time concentration monitoring. While the commercially available SPR biosensor has some of these capabilities, a nanoparticle based biosensor could improve both medical diagnostics and biomedical research by easily diagnosing large numbers of biomolecules quickly.

ACKNOWLEDGEMENTS

We acknowledge support of the Nanoscale Science and Engineering Initiative of the National Science Foundation under NSF Award Number EEC-0118025. Any opinions, findings and conclusions or recommendations expressed in this material are those of the authors and do not necessarily reflect those of the National Science Foundation. A. J. Haes also wishes to acknowledge the American Chemical Society Division of Analytical Chemistry and Dupont for a graduate fellowship. We also acknowledge research collaboration from Jonathan C. Riboh and Adam D. McFarland.

REFERENCES

1. A. P. F. Turner, "Biosensors--Sense and Sensitivity," *Science* **290**, pp. 1315-1317, 2000.
2. I. M. Klotz, *Ligand-Receptor Energetics: A Guide for the Perplexed.*, Wiley, New York, N. Y., 1997.
3. D. Hall, "Use of optical biosensors for the study of mechanistically concerted surface adsorption processes," *Anal. Biochem.* **288**, pp. 109-125, 2001.
4. H. J. Lee, T. T. Goodrich and R. M. Corn, "SPR imaging measurements of 1-D and 2-D DNA microarrays created from microfluidic channels on gold thin films," *Anal. Chem.* **73**, pp. 5525-5531, 2001.
5. J. Wang, X. Cai, G. Rivas, H. Shiraishi, P. A. M. Farias and N. Dontha, " DNA Electrochemical Biosensor for the Detection of Short DNA Sequences Related to the Human Immunodeficiency Virus.," *Anal. Chem.* **68**, pp. 2629-2634, 1996.
6. H. T. Walterbeek and A. J. G. M. van der Meer, "A sensitive and quantitative biosensing method for the determination of γ-ray emitting radionuclides in surface water.," *J. Environ. Radioact.* **33**, pp. 237-254, 1996.
7. D. R. Thevenot, K. Toth, R. A. Durst and G. S. Wilson, "Electrochemical biosensors: recommended definitions and classification," *Biosens. Bioelectron.* **16**, pp. 121-131, 2001.
8. M. Mascini, I. Palchetti and G. Marrazza, "DNA electrochemical biosensors," *Fres. J. Anal. Chem.* **369**, pp. 15-22, 2001.
9. J. Horacek and P. Skladal, "Improved direct piezoelectric biosensors operating in liquid solution for the competitive label-free immunoassay of 2,4-dichlorophenoxyacetic acid.," *Anal. Chim. Acta* **347**, pp. 43-50, 1997.
10. R. C. Ebersole, J. A. Miller, J. R. Moran and M. D. Ward, "Spontaneously formed functionally active avidin monolayers on metal surfaces: a strategy for immobilizing biological reagents and design of piezoelectric biosensors.," *J. Am. Chem. Soc.* **112**, pp. 3239-3241, 1990.
11. M. M. Miller, P. E. Sheehan, R. L. Edelstein, C. R. Tamanaha, L. Zhong, S. Bounnak, L. J. Whitman and R. J. Colton, "A DNA array sensor utilizing magnetic microbeads and magnetoelectronic detection.," *J. Magn. Magn. Mater.* **225**, pp. 156-160, 2001.
12. Y. R. Chemla, H. L. Grossman, Y. Poon, R. McDermott, R. Stevens, M. D. Alper and J. Clarke, "Ultrasensitive magnetic biosensor for homogeneous immunoassay," *Proc. Natl. Acad. Sci.* **97**, pp. 26, 2000.
13. B. Kasemo, "Biological surface science.," *Curr. Opin. Solid State Mater. Sci.* **3**, pp. 451-459, 1998.
14. R. Raiteri, M. Grattarola, H.-J. Butt and P. Skladal, "Micromechanical cantilever-based biosensors," *Sens. Acts. B* **B79**, pp. 115-126, 2001.
15. D. L. Polla, A. G. Erdman, W. P. Robbins, D. T. Markus, J. Diaz-Diaz, R. Rizq, Y. Nam, H. T. Brickner, A. Wang and P. Krulevitch, "Microdevices in medicine.," *Annu. Rev. Biomed. Eng.* **2**, pp. 551-576, 2000.
16. T. Natsume, H. Nakayama and T. Isobe, "BIA-MS-MS: biomolecular interaction analysis for functional proteomics.," *Trends in Biotech.* **19**, pp. S28-S33, 2001.

17. M. D. Malinsky, K. L. Kelly, G. C. Schatz and R. P. Van Duyne, "Chain Length Dependence and Sensing Capabilities of the Localized Surface Plasmon Resonance of Silver Nanoparticles Chemically Modified with Alkanethiol Self-Assembled Monolayers," *J. Am. Chem. Soc.* **123**, pp. 1471-1482, 2001.
18. N. Nath and A. Chilkoti, "A colorimetric gold nanoparticle sensor to interrogate biomolecular interactions in real time on a surface.," *Anal. Chem.* **74**, pp. 504-509, 2002.
19. S. Connolly, S. Cobbe and D. Fitzmaurice, "Effects of ligand-receptor geometry and stoichiometry on protein-induced aggregation of biotin-modified colloidal gold.," *J. Phys. Chem. B* **105**, pp. 2222-2226, 2001.
20. Y. W. Cao, R. Jin and C. A. Mirkin, "DNA modified core-shell Ag/Au nanoparticles.," *J. Am. Chem. Soc.* **123**, pp. 7961-7962, 2001.
21. P. Englebienne, A. Van Hoonacker and M. Verhas, "High-throughput screening using the surface plasmon resonance effect of colloidal gold nanoparticles.," *Analyst* **126**, pp. 1645-1651, 2001.
22. D. Eck, C. A. Helm, N. J. Wagner and K. A. Vaynberg, "Plasmon Resonance Measurements of the Adsorption and Adsorption Kinetics of a Biopolymer onto Gold Nanocolloids.," *Langmuir* **17**, pp. 957-960, 2001.
23. C. L. Haynes and R. P. Van Duyne, "Nanosphere Lithography: A Versatile Nanofabrication Tool for Studies of Size-Dependent Nanoparticle Optics.," *J. Phys. Chem. B* **105**, pp. 5599-5611, 2001.
24. T. A. Taton, G. Lu and C. A. Mirkin, "Two-Color Labeling of Oligonucleotide Arrays via Size-Selective Scattering of Nanoparticle Probes.," *J. Am. Chem. Soc.* **123**, pp. 5164-5165, 2001.
25. J. J. Storhoff, A. A. Lazarides, R. C. Mucic, C. A. Mirkin, R. L. Letsinger and G. C. Schatz, "What Controls the Optical Properties of DNA-Linked Gold Nanoparticle Assemblies?," *J. Am. Chem. Soc.* **122**, pp. 4640-4650, 2000.
26. S. Connolly, S. N. Rao and D. Fitzmaurice, "Characterization of Protein Aggregated Gold Nanocrystals.," *J. Am. Chem. Soc.* **104**, pp. 4765-4776, 2000.
27. T. Okamoto, I. Yamaguchi and T. Kobayashi, "Local plasmon sensor with gold colloid monolayers deposited upon glass substrates.," *Opt. Lett.* **25**, pp. 372-374, 2000.
28. M. Himmelhaus and H. Takei, "Cap-shaped gold nanoparticles for an optical biosensor.," *Sens. Actuators, B* **B63**, pp. 24-30, 2000.
29. G. Bauer, F. Pittner and T. Schalkhammer, "Metal nano-cluster biosensors.," *Mikrochim. Acta* **131**, pp. 107-114, 1999.
30. H. Takei, "Biological sensor based on localized surface plasmon associated with surface-bound au/polystyrene composite microparticles.," *Proc. SPIE-Int. Soc. Opt. Eng.* **3515**, pp. 278-283, 1998.
31. P. Englebienne, "Use of colloidal gold surface plasmon resonance peak shift to infer affinity constants from the interactions between protein antigens and antibodies specific for single or multiple epitopes.," *Analyst* **123**, pp. 1599-1603, 1998.
32. G. Steiner, M. T. Pham, C. Kuhne and R. Salzer, "Surface plasmon resonance within ion-implanted silver clusters," *Fres. J. Anal. Chem.* **362**, pp. 9-14, 1998.
33. J. J. Storhoff, R. Elghanian, R. C. Mucic, C. A. Mirkin and R. L. Letsinger, "One-Pot Colorimetric Differentiation of Polynucleotides with Single Base Imperfections Using Gold Nanoparticle Probes.," *J. Am. Chem. Soc.* **120**, pp. 1959-1964, 1998.
34. R. Elghanian, J. J. Storhoff, R. C. Mucic, R. L. Letsinger and C. A. Mirkin, "Selective colorimetric detection of polynucleotides based on the distance-dependent optical properties of gold nanoparticles.," *Science* **227**, pp. 1078-1080, 1997.
35. C. A. Mirkin, R. L. Letsinger, R. C. Mucic and J. J. Storhoff, "A DNA-based method for rationally assembling nanoparticles into macroscopic materials.," *Nature* **382**, pp. 607- 609, 1996.
36. G. Kalyuzhny, A. Vaskevick, G. Ashkenasy and A. Shanzer, "UV/Vis Spectroscopy of Metalloporphyrin and Metallophthalocyanine Monolayers Self-Assembled on Ultrathin Gold Films.," *J. Phys. Chem. B* **104**, pp. 8238-8244, 2000.
37. A. Hilger, N. Cuppers, M. Tenfelde and U. Kreibig, "Surface and interface effects in the optical properties of silver nanoparticles.," *Eur. Phys. J. D* **10**, pp. 115-118, 2000.
38. G. Kalyuzhny, M. A. Schneeweiss, A. Shanzer, A. Vaskevich and I. Rubinstein, "Differential plasmon spectroscopy as a tool for monitoring molecular binding to ultrathin gold films," *J. Am. Chem. Soc.* **123**, pp. 3177-3178, 2001.
39. M. Sanekata and I. Suzuka, "Physical and chemical interface effects on Mie plasmon absorption of sodium nanoclusters passivated with CH4-nCln (n=1-4) molecules.," *Chem. Phys. Lett.* **323**, pp. 98-104, 2000.

40. A. Henglein and D. Meisel, "Spectrophotometric Observations of the Adsorption of Organosulfur Compounds on Colloidal Silver Nanoparticles.," *J. Phys. Chem. B* **102**, pp. 8364-8366, 1998.
41. U. Kreibig, M. Gartz and A. Hilger, "Mie resonances. Sensors for physical and chemical cluster interface properties.," *Ber. Bunsen-Ges.* **101**, pp. 1593-1604, 1997.
42. A. J. Haes and R. P. Van Duyne, "A Nanoscale Optical Biosensor: Sensitivity and Selectivity of an Approach Based on the Localized Surface Plasmon Resonance Spectroscopy of Triangular Silver Nanoparticles," *J. Am. Chem. Soc.* **124**, pp. 10596 - 10604, 2002.
43. A. J. Haes and R. P. Van Duyne, "A Highly Sensitive and Selective Surface-Enhanced Nanobiosensor," *Mat. Res. Soc. Symp. Proc.* **723**, pp. O3.1.1-O3.1.6, 2002.
44. J. C. Riboh, A. J. Haes, A. D. McFarland, C. R. Yonzon and R. P. Van Duyne, "A Nanoscale Optical Biosensor: Real-Time Immunoassay in Physiological Buffer Enabled by Improved Nanoparticle Adhesion," *J. Phys. Chem. B* **107**, pp. 1772-1780, 2003.
45. L. S. Jung, C. T. Campbell, T. M. Chinowsky, M. N. Mar and S. S. Yee, "Quantitative Interpretation of the Response of Surface Plasmon Resonance Sensors to Adsorbed Films.," *Langmuir* **14**, pp. 5636-5648, 1998.
46. L. S. Jung and C. T. Campbell, "Sticking Probabilities in Adsorption from Liquid Solutions: Alkylthiols on Gold.," *Phys. Rev. Lett.* **84**, pp. 5164-5167, 2000.
47. L. S. Jung and C. T. Campbell, "Sticking Probabilities in Adsorption of Alkanethiols from Liquid Ethanol Solution onto Gold.," *J. Phys. Chem. B* **104**, pp. 11168-11178, 2000.
48. L. S. Jung, K. E. Nelson, P. S. Stayton and C. T. Campbell, "Binding and Dissociation Kinetics of Wild-Type and Mutant Streptavidins on Mixed Biotin-Containing Alkylthiolate Monolayers," *Langmuir* **16**, pp. 9421-9432, 2000.
49. A. J. Haes, S. Zou, G. C. Schatz and R. P. Van Duyne, *In preparation* 2003.
50. J. C. Hulteen and R. P. Van Duyne, "Nanosphere Lithography: A Materials General Fabrication Process for Periodic Particle Array Surfaces," *J. Vac. Sci. Technol. A* **13**, pp. 1553-1558, 1995.
51. J. C. Hulteen, D. A. Treichel, M. T. Smith, M. L. Duval, T. R. Jensen and R. P. Van Duyne, "Nanosphere Lithography: Size-Tunable Silver Nanoparticle and Surface Cluster Arrays," *J. Phys. Chem. B* **103**, pp. 3854-3863, 1999.
52. R. Micheletto, H. Fukuda and M. Ohtsu, "A Simple Method for the Production of a Two-Dimensional, Ordered Array of Small Latex Particles," *Langmuir* **11**, pp. 3333-3336, 1995.
53. C. Starr and R. Taggart, *Biology, The United and Diversity of Life*, Wadsworth Publishing Company, Belmont, CA, 1995.
54. N. M. Green, "**Avidin**," *Adv. Proten Chem.* **29**, pp. 85-133, 1975.
55. V. H. Perez-Luna, M. J. O'Brien, K. A. Opperman, P. D. Hampton, G. P. Lopez, L. A. Klumb and P. S. Stayton, "Molecular Recognition between Genetically Engineered Streptavidin and Surface-Bound Biotin.," *J. Am. Chem. Soc.* **121**, pp. 6469-6478, 1999.
56. M. Wilchek and E. A. Bayer, "Immobilized Biomolecules in Analysis," in *Avidin-biotin immobilization systems*, pp. 15-34, Oxford University Press, Oxford, UK, 1998.
57. M. Suzuki, F. Ozawa, S. Wakako and S. Aso, "Miniature surface-plasmon resonance immunosensors - rapid and repetitive procedure," *Anal. Bioanal. Chem.* **372**, pp. 301-304, 2002.
58. N. J. Lynch, R. K. Kilpatrick and R. G. Carbonell, "Aggregation of Ligand-Modified Liposomes by Specific Interactions with Proteins. II: Biotinylated Liposomes and Antibiotin Antibody," *Biotech. Bioeng.* **50**, pp. 169-183, 1996.
59. M. Adamczyk, P. G. Mattingly, K. Shreder and Z. Yu, "Surface Plasmon Resonance (SPR) as a Tool for Antibody Conjugate Analysis," *Bioconjugate Chem.* **10**, pp. 1032-1037, 1999.
60. P. Schuck, "Use of Surface Plasmon Resonance to Probe the Equilibrium and Dynamic Aspects of Interactions between Bilogical Macromolecules," *Annu. Rev. Biophys. Biomol. Struct.* **26**, pp. 541-566, 1997.
61. B. L. Frey and R. M. Corn, "Covalent Attachment and Derivatization of Poly(L-Lysine) Monolayers on Gold Surfaces as Characterized by Polarization-Modulation FT-IR Spectroscopy," *Anal. Chem.* **68**, pp. 3187-3193, 1996.
62. R. A. Copeland, S. P. A. Fodor and T. G. Spiro, "Surface-enhanced Raman spectra of an active flavoenzyme: glucose oxidase and riboflavin binding protein on silver particles," *J. Am. Chem. Soc.* **106**, pp. 3872-3874, 1984.

63. L. J. Freedman and M. T. Maddox, "A comparison of anti-biotin and biotinylated anti-avidin double-bridge and biotinylated tyramide immunohistochemical amplification," *J. Neuro. Meth.* **112**, pp. 43-49, 2001.
64. T. R. Jensen, G. C. Schatz and R. P. Van Duyne, "Nanosphere Lithography: Surface plasmon resonance spectrum of a periodic array of silver nanoparticles by UV-vis extinction spectroscopy and electrodynamic modeling," *J. Phys. Chem. B* **103**, pp. 2394-2401, 1999.
65. A. D. McFarland and R. P. Van Duyne, "Single Silver Nanoparticles as Real-Time Optical Sensors with Zeptomole Sensitivity," *Nano Letters* **In Press**, 2003.